A proton channel, Otopetrin 1 (OTOP1) is N-glycosylated at two asparagine residues in third extracellular loop

Omi Sasaki, Saori Yano-Nashimoto, and Soichiro Yamaguchi

Laboratory of Physiology, Department of Basic Veterinary Sciences, Faculty of Veterinary Medicine, Hokkaido University, Sapporo, Hokkaido, 060-0818, Japan

Correspondence:

Soichiro Yamaguchi, Laboratory of Physiology, Department of Basic Veterinary Sciences, Faculty of Veterinary Medicine, Hokkaido University, Sapporo, Hokkaido, 060-0818, Japan

Tel.: +81-11-706-5200

Fax: +81-11-706-5202

E-mail address: souya@vetmed.hokudai.ac.jp

Running title: OTOP1 is N-glycosylated

Abstract

A proton (H^+) channel, Otopetrin 1 (OTOP1) is an acid sensor in the sour taste receptor cells. Although OTOP1 is known to be activated by extracellular acid, no posttranslational modification of OTOP1 has been reported. As one of the posttranslational modifications, glycosylation is known to modulate many ion channels. In this study, we investigated whether OTOP1 is glycosylated and how the glycosylation affects OTOP1 function. Pharmacological and enzymatic examinations (using an N-glycosylation inhibitor, tunicamycin and peptide:N-glycanase F (PNGase F)) revealed that overexpressed mouse OTOP1 was N-glycosylated. As the N-glycans were Endoglycosidase H (Endo H)-sensitive, they were most likely high-mannose type. A site-directed mutagenesis approach revealed that both two asparagine residues (N238 and N251) in the third extracellular loop between the fifth transmembrane region and the sixth transmembrane region (L5-6) were the glycosylation sites. Prevention of the glycosylations by the mutations of the asparagine residues or by tunicamycin treatment diminished the whole-cell OTOP1 current densities. The results of cell surface biotinylation assay showed that the prevention of the glycosylations reduced the surface expression of OTOP1 at the plasma membrane. These results indicate that mouse OTOP1 is N-glycosylated at N238 and N251, and that the glycosylations are necessary for OTOP1 to show the maximum degree of H^+ current densities at the plasma membrane through promoting its targeting to the plasma membrane. These findings on glycosylations of OTOP1 will be a part of a comprehensive understanding on the regulations of OTOP1 function.

Keywords: Otopetrin 1, OTOP1, proton channel, glycosylation, cell surface protein

1 INTRODUCTION

Otopetrin 1 (OTOP1) was firstly identified as a membrane protein which was necessary for the otoconia formation in the inner ear (Hurle et al., 2003) and was more recently revealed to be a proton (H^+) selective channel, which is expressed in the sour (type III) taste receptor cells, and detects acidity and ammonium chloride (Liang, Wilson, Teng, Kinnamon, & Liman, 2023; Teng et al., 2019; Y.-H. Tu et al., 2018; Zhang et al., 2019). As a regulation of OTOP1 activity, it

has been known that extracellular acidity (acid strongly and alkali slightly) activates OTOP1 (Li et al., 2022; Teng et al., 2022; Tian et al., 2023). Zn^{2+} also not only inhibits OTOP1 but also activates OTOP1 (Fujii, Shimizu, Kaji, Katoh, & Sakai, 2023; Teng et al., 2023). However, thus far, no posttranslational modification of OTOP1 has been reported.

One of the posttranslational modifications is glycosylation. Proteins can be O-linked glycosylated and N-linked glycosylated in the ER and the Golgi apparatus. In the case of O-glycosylation, the oligosaccharides are attached to the protein via an oxygen atom on a serine (S) or threonine (T) residue (Lazniewska & Weiss, 2014). In the case of N-glycosylation, the saccharides are attached to an asparagine (N) residue located within a canonical sequence Asn-X-Thr/Ser (N-X-T/S, where X is any amino acid residue except proline) (Lazniewska & Weiss, 2014). It has been reported that glycosylation modulates more than 30 ion channels not only through controlling the proper folding of channel proteins but also controlling their targeting to the plasma membrane, channel gating, subunit heteromerization, and interaction with auxiliary subunits (Lazniewska & Weiss, 2014). However, no information on glycosylation of OTOP1 is available.

Therefore, in the present study, we investigated whether OTOP1 is glycosylated and concurrently which glycosylation (N-linked or O-linked, and type of N-glycosylation) occurs for OTOP1 by biochemical analyses. We also examined how the glycosylation affects OTOP1 function by measuring OTOP1 activity using a whole-cell patch clamp technique and by evaluating surface expression level of OTOP1 using a cell surface biotinylation assay.

2 MATERIALS AND METHODS

2.1 Plasmid and cell transfection

A full-length mouse *Otop1* was cloned in a pIRES2-EGFP (Clontech, Mountain View, CA, USA) vector or pmCherryC1 vector in the previous study (Islam, Sasaki, Yano-Nashimoto, Okamatsu-Ogura, & Yamaguchi, 2023). N-terminally 3×Flag-tagged *Otop1* was made using In-Fusion Snap Assembly Master Mix (Takara Bio, Otsu, Shiga, Japan) and cloned in a pcDNA3.1(+) vector (ThermoFisher, Waltham, MA, USA). Rat *Trpm5* was cloned in a pCMV-HA vector (Takara Bio) previously (Yamaguchi, Tanimoto, Iwasa, & Otsuguro, 2019). Mutants were produced using PrimeSTAR Mutagenesis Basal Kit (Takara Bio). The vectors were

transiently transfected into HEK293T cells or NIH3T3 cells (RIKEN BRC, Tsukuba, Ibaraki, Japan) using Trans-IT 293 transfection reagent or Trans-IT X2 transfection reagent (Takara Bio), respectively. In some experiments, the cells were treated with tunicamycin (Cayman Chemical Co., Ann Arbor, MI, USA), castanospermine (FUJIFILM Wako Chemicals, Osaka, Japan), or kifunensine (MedChemExpress, Monmouth Junction, NJ, USA) for 26-30 hours.

2.2 Western blot analysis

Thirty hours after the transfection, the transfected cells were lysed and treated with a urea sample buffer or Laemmli's sample buffer as described previously (Yamaguchi, Kamino, Hamamura, & Otsuguro, 2023). In some experiments, a part of the lysates was incubated with PNGase F (New England Biolabs (NEB), Ipswich, MA, USA), a mixture of O-Glycosidase (NEB) and Neuraminidase (NEB), or Endo H (NEB), following the manufacturer's instructions before the mixing with the urea sample buffer. Proteins were separated by SDS-PAGE and transferred to PVDF membranes. The membranes were blotted with anti-OTOP1 rabbit antibody (AHC-005, Alomone Labs, Jerusalem, Israel), anti-mCherry tag mouse antibody (E-AB-20015, Elabscience, Houston, TX, USA), anti-HA tag mouse antibody (M180-3S, MBL, Tokyo, Japan), anti-DYKDDDK (Flag) tag rabbit antibody (20543-1-AP, Proteintech, Rosemont, IL, USA), or anti-GFP rabbit antibody (E-AB-20050, Elabscience). The membranes were incubated with an HRP-conjugated anti-rabbit IgG or anti-mouse IgG secondary donkey antibody (Cytiva, Tokyo, Japan). β-actin was detected using an HRP-conjugated anti-β-actin antibody (Proteintech). The chemiluminescent signals were produced using Immobilon Forte Western HRP Substrate (Merck, Burlington, MA, USA), detected by a cooled CCD camera (BS-41L, Bitran, Gyoda, Saitama, Japan), and measured using ImageJ (Schneider, Rasband, & Eliceiri, 2012).

2.3 Cell surface biotinylation assay

The cell surface biotinylation assay was conducted as described previously (Yamaguchi et al., 2019) with some modifications. Briefly, 30 hours after the transfection, the transfected HEK293T cells were incubated with (Biotin +) or without (Biotin −) 0.5 ml 1.0 mg/ml EZ-link sulfo-NHS-s-s-biotin (ThermoFisher) in a biotinylation buffer (10 mM triethanolamine, 2 mM $CaCl_2$, 150 mM NaCl, pH 9.0 with HCl) for 15 minutes with gentle agitation at 4℃. After

washings, the cells were lysed and incubated with streptavidin-agarose beads (Merck). The beads were pelleted by a brief centrifugation. The supernatants were taken as the unbound intracellular fractions, mixed with a same volume of a urea sample buffer, and incubated at 37℃ for 10 minutes. After the beads were washed three times, the biotinylated proteins were eluted from the beads by mixing the beads with a urea sample buffer and heating the mixture at 37℃ for 10 minutes (surface fractions). The intracellular fractions and the surface fractions were analyzed by western blotting.

2.4 Co-immunoprecipitation

N-terminally 3×Flag-tagged OTOP1 and mCherry-tagged N238Q/N251Q OTOP1 mutant were co-expressed in HEK293T cells. For negative controls, empty vectors were used instead of each construct. The lysates of the cells were incubated with the anti-mCherry tag mouse antibody and protein A agarose beads (Santa Cruz Biotechnology, Dallas, TX, USA) at 4℃ overnight. After three washings, immunoprecipitated proteins were eluted by incubation with the urea sample buffer at 37℃ for 10 minutes and were analyzed by western blotting.

2.5 Whole-cell patch clamp measurement

Membrane currents were recorded from enhanced green fluorescence protein (EGFP)-positive single cells on the next day after the transfection. Whole-cell OTOP1 current measurements were conducted as described previously (Islam et al., 2023). To minimize pH alteration, the pipette solution contained a high concentration (200 mM) of a pH buffer, 4-(2-hydroxyethyl)piperazine-1-ethanesulfonic acid (HEPES) (pH 7.3 with cesium hydroxide (CsOH)). For bath solutions, N-methyl-D-glucamine (NMDG)-glutamate rich solutions were used. As pH buffers of bath solutions, HEPES was used for a pH 7.4 solution, 2-(N-morpholino)ethanesulfonic acid (MES) was used for pH 6.0-5.0 solutions, and citric acid was used for a pH 4.5 solution. The membrane potential was held at 0 mV and varied from −100 mV to +100 mV (with ramp pulse) over a duration of 400 msec following a prepulse of −100 mV for 50 msec every 5 seconds.

2.6 Statistical analysis

All average results are presented as means ± SEM of independent experiments (n). Two-tailed unpaired Student's t-test, paired t-test, and Dunnett's test were used to determine p-values. Statistical significance was defined as $p < 0.05$.

3 RESULTS

3.1 OTOP1 is N-glycosylated

When mouse OTOP1, which was expressed in HEK293T cells, was detected by western blotting, OTOP1 appeared as double bands (OTOP1, Figure 1a), which were not observed in empty-vector transfected cells (Empty vector, Figure 1a). We named the higher molecular weight band “Upper band” and the lower molecular weight band “Lower band”.

When the cells were treated with an N-glycosylation inhibitor, tunicamycin, for 26 hours before lysis, Upper band disappeared, and only Lower band remained (Tunicamycin, Figures 1b and 1c). These results suggest that OTOP1 is N-glycosylated and glycosylated OTOP1 appeared as Upper band.

To further examine which type of glycosylation the glycosylation of OTOP1 is (N-linked glycosylation or O-linked glycosylation), the extracted OTOP1 was treated with peptide:N-glycanase F (PNGase F), which cleaves the N-glycan, or the mixture of O-Glycosidase and neuraminidase, which cleaves the O-glycan. On one hand, with the treatment with O-glycosidase and neuraminidase, there was no difference in the double bands from control cells, which were treated without any enzymes (O-Glycosidase +Neuraminidase, Figures 1d and 1e). On the other hand, by the treatment with PNGase F, Upper band was diminished, and only Lower band appeared (PNGaseF, Figures 1d and 1e). Thus, the enzymatic examination also proved that OTOP1 was N-glycosylated. Additionally, Lower band seems to be unglycosylated OTOP1.

3.2 The N-glycans of OTOP1 are most likely high-mannose type

N-linked glycan structures are grouped into three types: high-mannose type, complex type, and hybrid type (Lazniewska & Weiss, 2014). To identify which type the N-glycosylations of OTOP1 are, we utilized inhibitors of N-glycosylation and Endoglycosidase H (Endo H) (Figure 2a, (Almahayni et al., 2022; Vagin, Turdikulova, & Sachs, 2004)). Endo H cleaves high-mannose

type and some hybrid type N-glycans while complex type N-glycan is resistant to its hydrolysis (Maley, Trimble, Tarentino, & Plummer, 1989). Firstly, after the 16 hours incubation of OTOP1 with Endo H at 37°C, Upper band almost disappeared and merged with Lower band (Figure 2b). The result indicates that the N-glycans of Upper band are not complex type. Secondly, by the treatment of the cells with castanospermine, an inhibitor of α-glucosidase I and II (Figure 2a), Upper band was shifted upward (Figure 2c). That means the N-glycans of Upper band were processed by α-glucosidase I and II from immature N-glycans (14-saccharide core). Finally, in order to examine whether the N-glycans of Upper band are high-mannose type or hybrid-type, we utilized a class I mannosidase inhibitor, kifunensine (Figure 2a) (Almahayni et al., 2022). If the position of Upper band is drastically shifted by the treatment with kifunensine, the N-glycans of Upper band are most likely hybrid-type. Additionally, if the N-glycans are high-mannose type and also trimmed by kifunensine-sensitive ER α1,2-mannosidase, which is related to ER-associated glycoprotein degradation, the position of Upper band might be shifted upward slightly (Ninagawa et al., 2014; Tremblay & Herscovics, 1999). Our results showed that the position of Upper band of OTOP1 was not affected by the treatment with kifunensine (Figure 2d). Therefore, the N-glycans of OTOP1 are most likely high-mannose type, and the high-mannose oligosaccharides were not trimmed by kifunensine-sensitive ER α1,2-mannosidase. To confirm that kifunensine inhibited the class I mannosidase in HEK293T cells, we examined the effect of kifunensine on overexpressed HA-tagged TRPM5, a non-selective cation channel. The N-glycan of TRPM5 has been reported to be complex type (Syam, Rougier, & Abriel, 2014). By the treatment with kifunensine, the higher molecular weight band of TRPM5 was shifted downward (Figure 2d). These results indicate that kifunensine inhibited class I mannosidase but did not affect the molecular weight of Upper band of OTOP1. Additionally, it was also shown that complex type N-glycosylation occurred in HEK293T cells. In conclusion, it was shown that the N-glycans of OTOP1 were most likely high-mannose type.

3.3 The glycosylation sites are 238th asparagine residue (N238) and 251st asparagine residue (N251)

The N-glycosylation occurs at asparagine residues which fulfill the consensus sequence: Asn-X-Thr/Ser (N-X-T/S, where X is any amino acid residue except proline) in the extracellular region (Marshall, 1972). Based on the criteria, there were three candidates for N-glycosylation

sites in mouse OTOP1, the membrane topology of which was predicted by TOPCONS (Bernsel, Viklund, Hennerdal, & Elofsson, 2009); 218th asparagine residue (N218), 238th asparagine residue (N238), and 251st asparagine residue (N251) in the third extracellular loop between the fifth transmembrane region and the sixth transmembrane region (L5-6) (Figure 3a). To reveal the N-glycosylation site of OTOP1, we made mutants where each asparagine was mutated to glutamine (Q), which cannot be glycosylated (Marshall, 1972).

The mutation of N218 did not affect the double bands of OTOP1 (N218Q, Figures 3b and 3c). Thus, N218 is not a glycosylation site. The mutations of N238 and N251 almost eliminated Upper band and caused the appearance of "Middle band" which was located between Upper band and Lower band (N238Q and N251Q, Figures 3b and 3c). As we assumed that the shift of Upper band to Middle band was due to the reduction in molecular weight by the loss of a glycosylation, and that both N238 and N251 were glycosylated, we made a double mutant where both N238 and N251 were mutated (N238Q/N251Q). The double mutation of N238 and N251 almost eliminated both Upper band and Middle band and left only Lower band (Figures 3b and 3c). These results revealed that N238 and N251 are the glycosylation sites of mouse OTOP1.

N238 and N251 are conserved in vertebrate OTOP1 (Figure 4a) and mouse OTOP3 (Figure 4b). In mouse OTOP2, only the first asparagine was conserved (Figure 4b). The high conservation of the glycosylation sites implies these glycosylations are important for the function of OTOP1.

We analyzed mouse OTOP1 but transfected HEK293T cells were a human cell line. To confirm that the same N-glycosylations of OTOP1 occur in mouse cells, we analyzed glycosylations of OTOP1 also using NIH3T3 cells, a mouse fibroblast cell line. In the case of NIH3T3 cells, we used mCherry-tagged OTOP1 because non-tagged OTOP1 was hardly detected due to its lower expression in NIH3T3 cells than that in HEK293T cells as well as the low titer of the anti-OTOP1 antibody used. The results of all experiments which we conducted (the treatments with PNGase F, Endo H, castanospermine, and kifunensine, and the double mutation of N238Q and N251Q) were practically the same as the results which were obtained using HEK293T cells (Supporting information S1). Therefore, the same N-glycosylations of OTOP1 occur not only in HEK293T cells but also in NIH3T3 cells.

OTOP1 forms a homo dimer (Saotome et al., 2019). As glycosylated OTOP1 and unglycosylated OTOP1 were simultaneously observed, we evaluated whether unglycosylated

OTOP1 can form a dimer with glycosylated OTOP1. We conducted a co-immunoprecipitation experiment using mCherry-tagged N238Q/N251Q mutant OTOP1 and 3×Flag-tagged wild type OTOP1 (Supporting information S2). We used mCherry-tagged N238Q/N251Q mutant OTOP1 as an unglycosylated OTOP1 and co-transfected with 3×Flag-tagged wild type OTOP1, which can be glycosylated and unglycosylated. By immunoprecipitation of mCherry-tagged unglycosylated OTOP1 using the anti-mCherry antibody, both glycosylated and unglycosylated 3×Flag-tagged OTOP1 were co-immunoprecipitated. This result indicates that unglycosylated OTOP1 can form dimer not only with unglycosylated OTOP1 but also with glycosylated OTOP1.

3.4 The glycosylations are necessary for OTOP1 to show the maximum degree of H^+ current densities at the plasma membrane

To evaluate the functional influence of the glycosylations, we measured whole-cell OTOP1 currents of WT OTOP1 and the mutants (N238Q, N251Q, and N238Q/N251Q). N238Q and N251Q showed smaller current densities than WT but the differences were not significant (Figures 5a and 5b). However, the double mutant, N238Q/N251Q showed a significantly smaller current density than WT (Figures 5a and 5b). Moreover, the inhibition of glycosylation by tunicamycin significantly reduced OTOP1 current density (Figures 5c and 5d). These results indicate that the glycosylations are necessary for OTOP1 to show the maximum degree of H^+ current densities at the plasma membrane.

The 229th histidine of human OTOP1 (the 227th histidine of mouse OTOP1) in the third extracellular loop was reported to be a key residue for activation by extracellular acid (Li et al., 2022). As the glycosylation sites are near the histidine, we evaluated the influence of the glycosylations on the activation by extracellular acid. The mutation of N238 slightly reduced the relative extent of activation by pH 5.0, which was statistically significant, but there were no differences at other pH (Supporting information S3). Additionally, the mutation of N251 and the treatment with tunicamycin did not cause any differences in the relative extent of activation by extracellular acid (Supporting information S3). Therefore, it is suggested that the glycosylations did not play a crucial role for the activation of OTOP1 by extracellular acid. Furthermore, the slight reduction in the activation of N238Q mutant by pH 5.0 was probably not caused by the loss of glycosylation on N238 but rather caused by the mutation of 238th asparagine to glutamine.

3.5 Prevention of glycosylations reduces the surface expression of OTOP1 at the plasma membrane

The reduction in the activity of OTOP1 at the plasma membrane by the prevention of the glycosylations might be due to a reduction in the targeting of OTOP1 to the plasma membrane. Therefore, we evaluated the surface expression of OTOP1 by surface biotinylation assay. Both the double mutations of N238 and N251 (N238Q/N251Q) and the inhibition of glycosylation by tunicamycin significantly reduced the relative amount of surface OTOP1 protein in comparison to the intracellular OTOP1 protein (Figure 6). Therefore, the prevention of the glycosylations reduced the surface expression of OTOP1 at the plasma membrane, and the reduction in the surface expression may explain the reduction of the whole-cell OTOP1 current densities at least in part.

4 DISCUSSION

The present study revealed that OTOP1 is N-glycosylated at N238 and N251, and that the glycosylations are necessary for OTOP1 to show the maximum degree of H^+ current densities at the plasma membrane. The results of the cell surface biotinylation assay indicate that the reduction in the whole-cell OTOP1 current densities by tunicamycin treatment (about 37% reduction, Figure 5d) was attributed to the reduction in the surface expression by tunicamycin treatment (about 57% reduction, Figure 6d) although it cannot be fully denied that the single channel activity of OTOP1 was also affected by the glycosylation. On the other hand, the reduction in the whole-cell OTOP1 current densities by N238Q/N251Q double mutation (about 79% reduction, Figure 5b) was more profound than those by tunicamycin treatment (about 37% reduction, Figure 6b) and the reduction in the surface expression of OTOP1 at the plasma membrane by the same mutations (about 53% reduction, Figure 6d). It might be because the double mutation of the asparagine residues to glutamine residues themselves affected the channel activity in addition to the loss of glycosylation and reduced not only the surface expression but also the single channel activity of OTOP1. Thus far, the single channel recording of OTOP1 has not been reported probably due to a technical difficulty caused by a small single channel conductance of OTOP1, which was also discussed elsewhere (Teng et al., 2022). However, if

possible, such analyses would be useful for the deeper understanding of OTOP1 regulation by glycosylation.

N218 was not a glycosylation site. We used a membrane topology of OTOP1 predicted by TOPCONS (Bernsel et al., 2009), but a mouse OTOP1 structure which was predicted by AlphaFold (UniProt accession number: Q80VM9) (Jumper et al., 2021) indicates that the alpha helix forming the fifth transmembrane region continues to 234th leucine. Therefore, although N238 and N251 are predicted to be placed in L5-6, N218 is supposed to be in the alpha helix. That is probably one of the reasons why N218 is not glycosylated.

Intriguingly, Middle band was negligible and almost only Upper band and Lower band were observed in the lanes of WT OTOP1 and Control (e.g. Figure 3b). That means both asparagine residues (N238 and N251) are always glycosylated when OTOP1 is glycosylated and neither of them is glycosylated when OTOP1 is not glycosylated. Moreover, both unglycosylated Lower band and glycosylated Upper band were always observed, even in the surface fraction of the cell surface biotinylation assay (Figures 6a and 6c). As unglycosylated OTOP1 can form a dimer not only with unglycosylated OTOP1 but also with glycosylated OTOP1 (Supporting information S2), the dimer between unglycosylated OTOP1 and glycosylated OTOP1 might be a part of the reason why both unglycosylated OTOP1 and glycosylated OTOP1 were observed on the surface of the cells. However, the mechanism underlying the existence of the unglycosylated OTOP1 is unknown. Further experiments are required to reveal the details of the mechanisms underlying the glycosylations on each glycosylation site.

Additionally, unglycosylated OTOP1 (N238Q/N251Q mutant and OTOP1 in tunicamycin treated cells) also showed whole-cell OTOP1 currents and surface expression although they were relatively small (Figures 5 and 6). These results indicate that unglycosylated OTOP1 can function as a proton channel and can be transported to the plasma membrane to a certain extent. Therefore, it is suggested that the glycosylations of OTOP1 are not essential for its activity.

The N-glycans of OTOP1 were suggested to be high-mannose type (Figure 2 and Supporting information S1). Although complex type is the dominant form of N-linked glycosylation in mammals (Abdelbary & Nolz, 2023), there are several reports that high-mannose type N-glycosylated proteins also reach the cell surface. For example, the amounts of high-mannose type N-glycans on the cell surface of HEK293 cells and CHO (Chinese Hamster Ovary)-

K1 cells were reported to be about 10% and 42% of total N-glycans on the cell surface, respectively (Hamouda et al., 2014). Additionally, not only complex type N-glycosylated proteins but also a smaller amount of high-mannose type N-glycosylated proteins can reach the plasma membrane in the case of certain glycoproteins, such as GluA1, GluN2B, intercellular adhesion molecule-1, TGF-β receptor, Basigin, TRPM5, and others (Cui, Yamamoto, & Ikeda, 2024; Hanus et al., 2016; Kim, Park, Lee, Lee, & Kim, 2012; Regal-McDonald, Xu, Barnes, & Patel, 2019; Syam et al., 2014). Furthermore, the N-glycans of GluN1 and $GABA_A$ receptor β3 subunit were reported to be entirely high-mannose type (Hanus et al., 2016). Although environmental factors (e.g., expression level of glycosidases/glycosyltransferases) might cause such a lack of processing of high-mannose type N-glycan (Suga, Nagae, & Yamaguchi, 2018), the environmental factors do not seem to be the reason why the N-glycans of OTOP1 were not processed in this study. That is because the N-glycan of TRPM5, which was similarly expressed in the same cell line, was normally processed and became complex type (Figure 2 and Supporting information S1). Instead of the environmental factors, intrinsic structural factors around N-glycosylation sites are suggested to influence glycan processing and maturation (Suga et al., 2018) as there are examples that certain N-glycan(s) among several N-glycans in a glycoprotein remained high-mannose type site-specifically (Kv3.1b, transferrin receptor, and avian serum IgG (Hayes, Williams, Costello, Enns, & Lucas, 1995; Suzuki & Lee, 2004; Vicente et al., 2018)). A study on the local structural properties of N-glycosylation sites using the 3D structural data deposited in the Protein Data Bank revealed that γ-branched amino acid residues (Asn (N), Asp (D), and Leu (L)) and Ile (I) occurred more frequently around immature (including high-mannose type) N-glycans (Suga et al., 2018). Around the N-glycosylation sites of OTOP1 (N238 and N251), there are a large number of these amino acid residues (Figure 4, e.g. L234, I239, I240, L242, D243, D244, L257). These amino acid residues of OTOP1 might impede the processing of the N-glycans. Therefore, although further investigations are required, OTOP1 might be a useful model for the study on the structural determinants of N-glycoprotein processing.

OTOP1 has been reported to be expressed in the inner ear, taste bud, and brown adipose tissue (Hurle et al., 2003; Y.-H. Tu et al., 2018; Y. H. Tu, Liu, Xiao, Gavrilova, & Reitman, 2023). The cell type specific N-glycosylation pattern might provide a cell-specific difference in OTOP1 function although we proved that same N-glycosylations of mouse OTOP1 occurred in a human cell line and a mouse cell line (Supplementary information S1). Therefore, the evaluation of the N-glycan structure of OTOP1 in each tissue would be an interesting research topic.

Finally, the structure-function relationships of OTOP1 have been extensively investigated (Li et al., 2022; Liang et al., 2023; Saotome et al., 2019; Teng et al., 2023, 2022; Tian et al., 2023). To fully understand the structure-function relationships of OTOP1, the glycosylations on N238 and N251 will be a factor which needs to be considered. Furthermore, glycosylation can affect channel function through affecting association with other subunits (Lazniewska & Weiss, 2014). Although no interacting protein of OTOP1 has been discovered, if any exist, the glycosylations of OTOP1 might affect the association between OTOP1 and its interacting protein. In conclusion, the findings on the glycosylations of OTOP1 in the present study will be a part of the comprehensive understanding on OTOP1 function.

Acknowledgments

This work was supported by Lotte Foundation (to S.Y.), Koyanagi Foundation (to S.Y.) and JSPS KAKENHI Grant Number 22K06825 (to S.Y.).

REFERENCES

Abdelbary, M., & Nolz, J. C. (2023). N-linked glycans: An underappreciated key determinant of T cell development, activation, and function. *Immunometabolism (United States)*, *5*(4), E00035. https://doi.org/10.1097/IN9.0000000000000035

Almahayni, K., Spiekermann, M., Fiore, A., Yu, G., Pedram, K., & Möckl, L. (2022). Small molecule inhibitors of mammalian glycosylation. *Matrix Biology Plus*, *16*. https://doi.org/10.1016/j.mbplus.2022.100108

Bernsel, A., Viklund, H., Hennerdal, A., & Elofsson, A. (2009). TOPCONS: Consensus prediction of membrane protein topology. *Nucleic Acids Research*, *37*(SUPPL. 2), 465–468. https://doi.org/10.1093/nar/gkp363

Cui, D., Yamamoto, K., & Ikeda, E. (2024). High-Mannose–Type Glycan of Basigin in Endothelial Cells Is Essential for the Opening of the Blood–Brain Barrier Induced by Hypoxia, Cyclophilin A, or Tumor Necrosis Factor-α. *American Journal of Pathology*, *194*(4), 612–625. https://doi.org/10.1016/j.ajpath.2023.11.007

Fujii, T., Shimizu, T., Kaji, Y., Katoh, M., & Sakai, H. (2023). Activation of mouse Otop3

proton channels by Zn^{2+}. *Biochemical and Biophysical Research Communications*, *658*, 55–61. https://doi.org/10.1016/j.bbrc.2023.03.066

Hamouda, H., Kaup, M., Ullah, M., Berger, M., Sandig, V., Tauber, R., & Blanchard, V. (2014). Rapid analysis of cell surface N-glycosylation from living cells using mass spectrometry. *Journal of Proteome Research*, *13*(12), 6144–6151. https://doi.org/10.1021/pr5003005

Hanus, C., Geptin, H., Tushev, G., Garg, S., Alvarez-Castelao, B., Sambandan, S., … Schuman, E. M. (2016). Unconventional secretory processing diversifies neuronal ion channel properties. *ELife*, *5*, 1–27. https://doi.org/10.7554/elife.20609

Hayes, G. R., Williams, A., Costello, C. E., Enns, C. A., & Lucas, J. J. (1995). The critical glycosylation site of human transferrin receptor contains a high-mannose oligosaccharide. *Glycobiology*, *5*(2), 227–232. https://doi.org/10.1093/glycob/5.2.227

Hurle, B., Ignatova, E., Massironi, S. M., Mashimo, T., Rios, X., Thalmann, I., … Ornitz, D. M. (2003). Non-syndromic vestibular disorder with otoconial agenesis in tilted/mergulhador mice caused by mutations in otopetrin 1. *Human Molecular Genetics*, *12*(7), 777–789. https://doi.org/10.1093/hmg/ddg087

Islam, M. M., Sasaki, O., Yano-Nashimoto, S., Okamatsu-Ogura, Y., & Yamaguchi, S. (2023). Cibacron blue 3G-A is a novel inhibitor of Otopetrin 1 (OTOP1), a proton channel. *Biochemical and Biophysical Research Communications*, *665*, 64–70. https://doi.org/10.1016/j.bbrc.2023.04.112

Jumper, J., Evans, R., Pritzel, A., Green, T., Figurnov, M., Ronneberger, O., … Hassabis, D. (2021). Highly accurate protein structure prediction with AlphaFold. *Nature*, *596*(7873), 583–589. https://doi.org/10.1038/s41586-021-03819-2

Kim, Y. W., Park, J., Lee, H. J., Lee, S. Y., & Kim, S. J. (2012). TGF-β sensitivity is determined by N-linked glycosylation of the type II TGF-β receptor. *Biochemical Journal*, *445*(3), 403–411. https://doi.org/10.1042/BJ20111923

Lazniewska, J., & Weiss, N. (2014). The “sweet” side of ion channels. *Reviews of Physiology, Biochemistry and Pharmacology*, *167*, 67–114. https://doi.org/10.1007/112_2014_20

Li, B., Wang, Y., Castro, A., Ng, C., Wang, Z., Chaudhry, H., … Yu, Y. (2022). The roles of two extracellular loops in proton sensing and permeation in human Otop1 proton channel. *Communications Biology*, *5*(1). https://doi.org/10.1038/s42003-022-04085-2

Liang, Z., Wilson, C. E., Teng, B., Kinnamon, S. C., & Liman, E. R. (2023). The proton channel OTOP1 is a sensor for the taste of ammonium chloride. *Nature Communications*, *14*(1). https://doi.org/10.1038/s41467-023-41637-4

Maley, F., Trimble, R. B., Tarentino, A. L., & Plummer, T. H. (1989). Characterization of glycoproteins and their associated oligosaccharides through the use of endoglycosidases. *Analytical Biochemistry*, *180*(2), 195–204. https://doi.org/10.1016/0003-2697(89)90115-2

Marshall, R. (1972). GLYCOPROTEINS. *Annu. Rev. Biochem*, *41*(34), 673–702.

Ninagawa, S., Okada, T., Sumitomo, Y., Kamiya, Y., Kato, K., Horimoto, S., … Mori, K. (2014). EDEM2 initiates mammalian glycoprotein ERAD by catalyzing the first mannose trimming step. *Journal of Cell Biology*, *206*(3), 347–356. https://doi.org/10.1083/jcb.201404075

Regal-McDonald, K., Xu, B., Barnes, J. W., & Patel, R. P. (2019). High-mannose intercellular adhesion molecule-1 enhances CD16+ monocyte adhesion to the endothelium. *American Journal of Physiology - Heart and Circulatory Physiology*, *317*(5), H1028–H1038. https://doi.org/10.1152/AJPHEART.00306.2019

Saotome, K., Teng, B., Tsui, C. C. (Alex), Lee, W. H., Tu, Y. H., Kaplan, J. P., … Ward, A. B. (2019). Structures of the otopetrin proton channels Otop1 and Otop3. *Nature Structural and Molecular Biology*, *26*(6), 518–525. https://doi.org/10.1038/s41594-019-0235-9

Schneider, C. A., Rasband, W. S., & Eliceiri, K. W. (2012). NIH Image to ImageJ: 25 years of image analysis. *Nature Methods*, *9*(7), 671–675. https://doi.org/10.1038/nmeth.2089

Suga, A., Nagae, M., & Yamaguchi, Y. (2018). Analysis of protein landscapes around N-glycosylation sites from the PDB repository for understanding the structural basis of N-glycoprotein processing and maturation. *Glycobiology*, *28*(10), 774–785. https://doi.org/10.1093/glycob/cwy059

Suzuki, N., & Lee, Y. C. (2004). Site-specific N-glycosylation of chicken serum IgG. *Glycobiology*, *14*(3), 275–292. https://doi.org/10.1093/glycob/cwh031

Syam, N., Rougier, J. S., & Abriel, H. (2014). Glycosylation of TRPM4 and TRPM5 channels: Molecular determinants and functional aspects. *Frontiers in Cellular Neuroscience*, *8*(52), 1–12. https://doi.org/10.3389/fncel.2014.00052

Teng, B., Kaplan, J. P., Liang, Z., Chyung, K. S., Goldschen-Ohm, M. P., & Liman, E. R. (2023). Zinc activation of OTOP proton channels identifies structural elements of the

gating apparatus. *ELife*, *12*, 1–21. https://doi.org/10.7554/eLife.85317

Teng, B., Kaplan, J. P., Liang, Z., Krieger, Z., Tu, Y. H., Burendei, B., … Liman, E. R. (2022). Structural motifs for subtype-specific pH-sensitive gating of vertebrate otopetrin proton channels. *ELife*, *11*, 1–19. https://doi.org/10.7554/eLife.77946

Teng, B., Wilson, C. E., Tu, Y. H., Joshi, N. R., Kinnamon, S. C., & Liman, E. R. (2019). Cellular and Neural Responses to Sour Stimuli Require the Proton Channel Otop1. *Current Biology*, *29*(21), 3647-3656.e5. https://doi.org/10.1016/j.cub.2019.08.077

Tian, L., Zhang, H., Yang, S., Luo, A., Kamau, P. M., Hu, J., … Lai, R. (2023). Vertebrate OTOP1 is also an alkali-activated channel. *Nature Communications*, *14*(1). https://doi.org/10.1038/s41467-022-35754-9

Tremblay, L. O., & Herscovics, A. (1999). Cloning and expression of a specific human α1,2-mannosidase that trims Man9GlcNAc2 to Man8GlcNAc2 isomer B during N-glycan biosynthesis. *Glycobiology*, *9*(10), 1073–1078. https://doi.org/10.1093/glycob/9.10.1073

Tu, Y.-H., Cooper, A. J., Teng, B., Chang, R. B., Artiga, D. J., Turner, H. N., … Liman, E. R. (2018). An evolutionarily conserved gene family encodes proton-selective ion channels. *Science (New York, N.Y.)*, *359*(6379), 1047–1050. https://doi.org/10.1126/science.aao3264

Tu, Y. H., Liu, N., Xiao, C., Gavrilova, O., & Reitman, M. L. (2023). Loss of Otopetrin 1 affects thermoregulation during fasting in mice. *PLoS ONE*, *18*(10), e0292610. https://doi.org/10.1371/journal.pone.0292610

Vagin, O., Turdikulova, S., & Sachs, G. (2004). The H,K-ATPase β subunit as a model to study the role of N-glycosylation in membrane trafficking and apical sorting. *Journal of Biological Chemistry*, *279*(37), 39026–39034. https://doi.org/10.1074/jbc.M405453200

Vicente, P. C., Kim, J. Y., Ha, J. J., Song, M. Y., Lee, H. K., Kim, D. H., … Park, K. S. (2018). Identification and characterization of site-specific N-glycosylation in the potassium channel Kv3.1b. *Journal of Cellular Physiology*, *233*(1), 549–558. https://doi.org/10.1002/jcp.25915

Yamaguchi, S., Kamino, M., Hamamura, M., & Otsuguro, K. I. (2023). The cytosolic N-terminal region of heterologously-expressed transmembrane channel-like protein 1 (TMC1) can be cleaved in HEK293 cells. *PLoS ONE*, *18*(6), e0287249. https://doi.org/10.1371/journal.pone.0287249

Yamaguchi, S., Tanimoto, A., Iwasa, S., & Otsuguro, K. I. (2019). TRPM4 and TRPM5

channels share crucial amino acid residues for Ca^{2+} sensitivity but not significance of $PI(4,5)P_2$. *International Journal of Molecular Sciences*, *20*(8), 2012. https://doi.org/10.3390/ijms20082012

Zhang, J., Jin, H., Zhang, W., Ding, C., O'Keeffe, S., Ye, M., & Zuker, C. S. (2019). Sour Sensing from the Tongue to the Brain. *Cell*, *179*(2), 392-402.e15. https://doi.org/10.1016/j.cell.2019.08.031

Figure Legends

Figure 1

Pharmacological and enzymatic examinations revealed that OTOP1 was N-glycosylated. (a) A representative result (out of three blots) of western blot analysis for OTOP1 (upper) or EGFP (lower). The three bands which were also observed in empty-vector (pIRES2-EGFP) transfected HEK293T cells (Empty vector) are nonspecific bands. The higher molecular weight band of OTOP1 was labeled as Upper band, and the lower one was labeled as Lower band. EGFP was detected to monitor transfection efficiencies. (b) HEK293T cells which expressed OTOP1 were treated with 2.0 μg/ml tunicamycin, an N-glycosylation inhibitor (Tunicamycin) or with its solvent, dimethyl sulfoxide (DMSO, 0.02%) (Control) for 26 hours before lysis. (c) The band intensities of Upper band and Lower band of OTOP1 were measured, and the proportions of Upper band in Control and Tunicamycin were calculated and illustrated as a bar graph. Shown are mean ± SEM. *: $p < 0.05$ (Dunnett's test, vs Control, n = 3). (d) A representative result (out of three blots) of western blot analysis for OTOP1, that was treated with enzymes which remove glycans. To detect intact OTOP1, which was not exposed by any extra-treatment, the lysates of HEK293T cells expressing OTOP1 (Non-treated) and HEK293T cells which were transfected with the empty vector (Empty vector) were loaded. The remaining lysates of HEK293T expressing OTOP1 were treated with distilled water (Control), 25 U/μl peptide:N-glycanase F (PNGase F), or the mixture of 1,000 U/μl O-Glycosidase and 12.5 U/μl Neuraminidase (O-Glycosidase +Neuraminidase) at 37°C for 1 hour. The arrows indicating bands are the same as those in Figure 1a. (e) The band intensities of Upper band and Lower band of OTOP1 were measured, and the proportions of Upper band in Control, PNGase F, and O-Glycosidase +Neuraminidase were calculated and illustrated as a bar graph. Shown are mean ± SEM. *: $p < 0.05$ (Dunnett's test, vs Control, n = 3).

Figure 2

The N-glycans of OTOP1 are most likely high-mannose type. (a) A simplified sequence of N-glycan biosynthesis, and inhibitors and glycosidases of N-glycosylation. Tunicamycin inhibits the formation of N-acetylglucosamine-lipid intermediates. Castanospermine inhibits trimming of initially attached 14-saccharide core, an immature glycan. Kifunensine prevents the formation of

hybrid type N-glycan and complex type N-glycan by inhibiting further trimming of mannose from high-mannose type N-glycan. Endo H cleaves high-mannose type N-glycan and some hybrid type N-glycan. PNGase F cleaves all types of N-glycan. (b) A representative result of a treatment with Endo H. After lysis of the OTOP1 expressing cells, the lysates were incubated with 50 U/μl Endo H at 37°C for 16 hours (Endo H) or without it (Control). To confirm the position of the intact OTOP1, which was not exposed by any extra-treatment, the lysate of HEK293T cells expressing OTOP1 (Non-treated) and the lysate of HEK293T cells which were transfected with an empty vector (Empty vector) were loaded. (c) The OTOP1 expressing HEK293T cells were incubated with 100 μg/ml castanospermine, an α/β-glucosidase inhibitor (Castanospermine) or without it (Control) for 30 hours from just before transfection. (d) The OTOP1 expressing HEK293T cells were incubated with 50 μM kifunensine, an inhibitor of class I α-mannosidases (Kifunensine), or without it (Control) for 30 hours from just before transfection, and OTOP1 was detected (left). To confirm that 50 μM kifunensine inhibited class I α-mannosidases of the cells, HA-tagged rat TRPM5 expressing HEK293T cells were incubated with 50 μM kifunensine, and TRPM5 was detected using an anti-HA antibody (right). All experiments were repeated three times.

Figure 3

OTOP1 was glycosylated at 238th asparagine residue (N238) and 251st asparagine residue (N251). (a) A membrane topology of OTOP1, which was predicted by TOPCONS (Bernsel et al., 2009). The arrows indicate the positions of three candidate asparagine residues (218th asparagine (N218), N238, and N251) which fulfill the N-glycosylation consensus sequence (Asn-X-Thr/Ser, N-X-T/S, where X is any amino acid residue except proline) in the extracellular region. (b) A representative result (out of three blots) of western blot analysis for OTOP1 (upper) or EGFP (lower). HEK293T cells were transfected with an empty vector (Empty vector) or expressed wild-type OTOP1 (WT), N218Q mutant (N218Q), N238Q mutant (N238Q), N251Q mutant (N251Q), or N238Q and N251Q double mutant (N238Q/N251Q). In addition to Upper band and Lower band, N238Q and N251Q showed Middle band between Upper band and Lower band. (c) The band intensities of Upper band, Middle band, and Lower band of OTOP1 were measured, and the proportions of Upper band (left) or Middle band (right) in WT, N218Q, N238Q, N251Q, and N238Q/N251Q were calculated and illustrated as a bar graph. Shown are mean ± SEM. *: $p < 0.05$, ***: $p < 0.001$ (Dunnett's test, vs WT, n = 3).

Figure 4

The N-glycosylated asparagine residues (N238 and N251) are conserved in vertebrate OTOP1 and other OTOP family members (OTOP2 and OTOP3). (a) An amino acid sequence alignment of the third extracellular loop between the fifth transmembrane region (TM5) and the sixth transmembrane region (TM6) of several vertebrate OTOP1. Binominal names and Genbank accession numbers of the vertebrate OTOP1 are as follows: mouse: *Mus musculus*; NP_766297.2, human: *Homo sapiens*; NP_819056.1, rat: *Rattus norvegicus*; NP_852098.1, bovine: *Bos taurus*; NP_001193713.1, sheep: *Ovis aries*; XP_014951783.2, dog: *Canis lupus familiaris*; XP_03389628, cat: *Felis catus*; XP_023109080, hamster: *Phodopus roborovskii*; CAH6975926.1, hedgehog: *Erinaceus europaeus*; XP_060044452.1, dolphin: *Lagenorhynchus albirostris*; XP_060003039, pigeon: *Columba livia*; KAK2541027.1, chicken: *Gallus gallus*; XP_040528877.1, snake: *Pantherophis guttatus*; XP_034288795, frog: *Xenopus laevis*; XP_018124006, zebrafish: *Danio rerio*; NP_942098.1. Asparagine (N) and threonine or serine (T/S) which correspond to the consensus sequences of N238 and N251 of mouse OTOP1 are written in red bold letters. (b) An amino acid sequence alignment of the third extracellular loop of mouse OTOP1, mouse OTOP2 (NP_001334576.1), and mouse OTOP3 (NP_001334576.1). N and T/S which correspond to the consensus sequences of N238 and N251 of mouse OTOP1 are written in red bold letters.

Figure 5

Prevention of glycosylation reduced whole-cell OTOP1 current density. (a) Representative current-voltage (I-V) plots of whole-cell current densities which were measured from HEK293T cells expressing WT OTOP1 or mutant OTOP1 (N238Q, N251Q, and N238Q/N251Q) at pH 7.4 (black line) or pH 5.5 (green line). (b) A summary of current density magnitudes of WT OTOP1 and mutant OTOP1 (N238Q, N251Q, and N238Q/N251Q) at –100 mV, evoked by a pH 5.5 solution [(current density at pH 7.4) – (current density at pH 5.5)]. Shown are mean ± SEM. ***: $p < 0.001$ (Dunnett's test, vs WT, n = 10 to 16). (c) Representative I-V plots of whole-cell OTOP1 current densities which were measured at pH 7.4 (black line) or pH 5.5 (green line) from HEK293T cells treated with 2.0 μg/ml tunicamycin (Tunicamycin) or its solvent, 0.02% DMSO

(Control) for 26 hours. (d) A summary of current density magnitudes evoked by a pH 5.5 solution at –100 mV. Cells were treated with tunicamycin (Tunicamycin) or DMSO (Control). Shown are mean ± SEM. *: $p < 0.05$ (unpaired Student's t-test, n = 13 or 14).

Figure 6

Prevention of glycosylation reduced surface expression of OTOP1. (a) A representative result (out of five blots) of a cell surface biotinylation assay of WT OTOP1 and N238Q/N251Q mutant. The left half of the membrane shows surface fractions, and the right half shows intracellular fractions. HEK293T cells expressed WT OTOP1 or N238Q/N251Q mutant, or were transfected with an empty vector. To monitor nonspecific binding to avidin beads, non-biotinylated cell lysates (Biotin –) were pulled down in addition to biotinylated cell lysates (Biotin +). In the upper membrane, OTOP1 was detected. In the lower membrane, β-actin was detected to confirm negligible leakage of intracellular proteins into the surface fractions. (b) A summary of the ratios of OTOP1 proteins (WT OTOP1 or N238Q/N251Q) in the surface fraction to those in the intracellular fraction. Shown are mean ± SEM. *: $p < 0.05$ (paired t-test, n = 5). (c) A representative result (out of four blots) of a cell surface biotinylation assay of WT OTOP1 in the HEK293T cells which were treated with 2.0 μg/ml tunicamycin (Tunicamycin) or its solvent, 0.02% DMSO (Control), for 26 hours. Others are same in (a). (d) A summary of the signal ratios of OTOP1 proteins in the surface fraction of control cells or tunicamycin-treated cells to OTOP1 proteins in the intracellular fraction. Shown are mean ± SEM. **: $p < 0.01$ (paired t-test, n = 4).

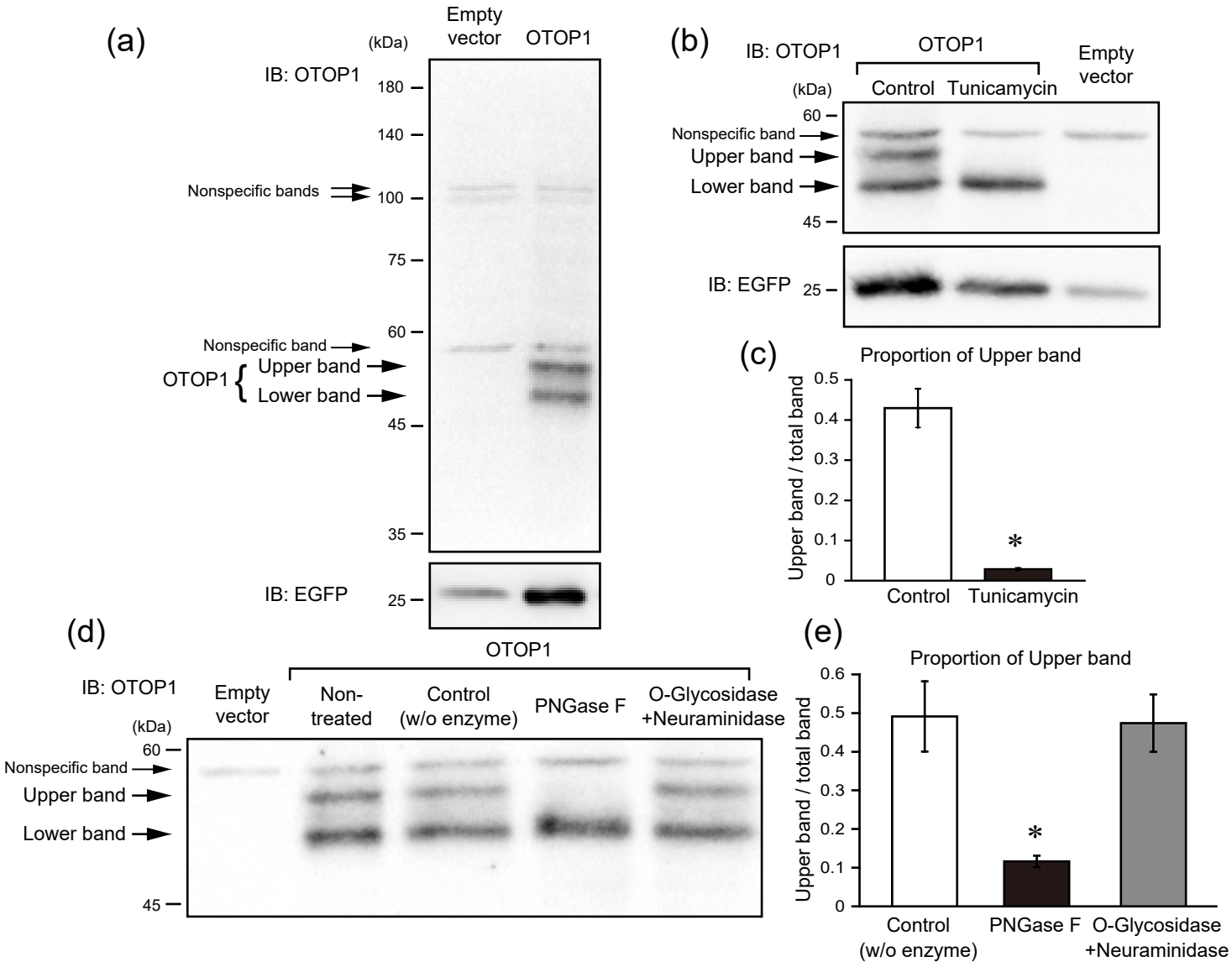

Figure 1

Pharmacological and enzymatic examinations revealed that OTOP1 was N-glycosylated. (a) A representative result (out of three blots) of western blot analysis for OTOP1 (upper) or EGFP (lower). The three bands which were also observed in empty-vector (pIRES2-EGFP) transfected HEK293T cells (Empty vector) are nonspecific bands. The higher molecular weight band of OTOP1 was labeled as Upper band, and the lower one was labeled as Lower band. EGFP was detected to monitor transfection efficiencies. (b) HEK293T cells which expressed OTOP1 were treated with 2.0 µg/ml tunicamycin, an N-glycosylation inhibitor (Tunicamycin) or with its solvent, dimethyl sulfoxide (DMSO, 0.02%) (Control) for 26 hours before lysis. (c) The band intensities of Upper band and Lower band of OTOP1 were measured, and the proportions of Upper band in Control and Tunicamycin were calculated and illustrated as a bar graph. Shown are mean ± SEM. *: $p < 0.05$ (Dunnett's test, vs Control, n = 3). (d) A representative result (out of three blots) of western blot analysis for OTOP1, that was treated with enzymes which remove glycans. To detect intact OTOP1, which was not exposed by any extra-treatment, the lysates of HEK293T cells expressing OTOP1 (Non-treated) and HEK293T cells which were transfected with the empty vector (Empty vector) were loaded. The remaining lysates of HEK293T expressing OTOP1 were treated with distilled water (Control), 25 U/µl peptide:N-glycanase F (PNGase F), or the mixture of 1,000 U/µl O-Glycosidase and 12.5 U/µl Neuraminidase (O-Glycosidase +Neuraminidase) at 37℃ for 1 hour. The arrows indicating bands are the same as those in Figure 1a. (e) The band intensities of Upper band and Lower band of OTOP1 were measured, and the proportions of Upper band in Control, PNGase F, and O-Glycosidase +Neuraminidase were calculated and illustrated as a bar graph. Shown are mean ± SEM. *: $p < 0.05$ (Dunnett's test, vs Control, n = 3).

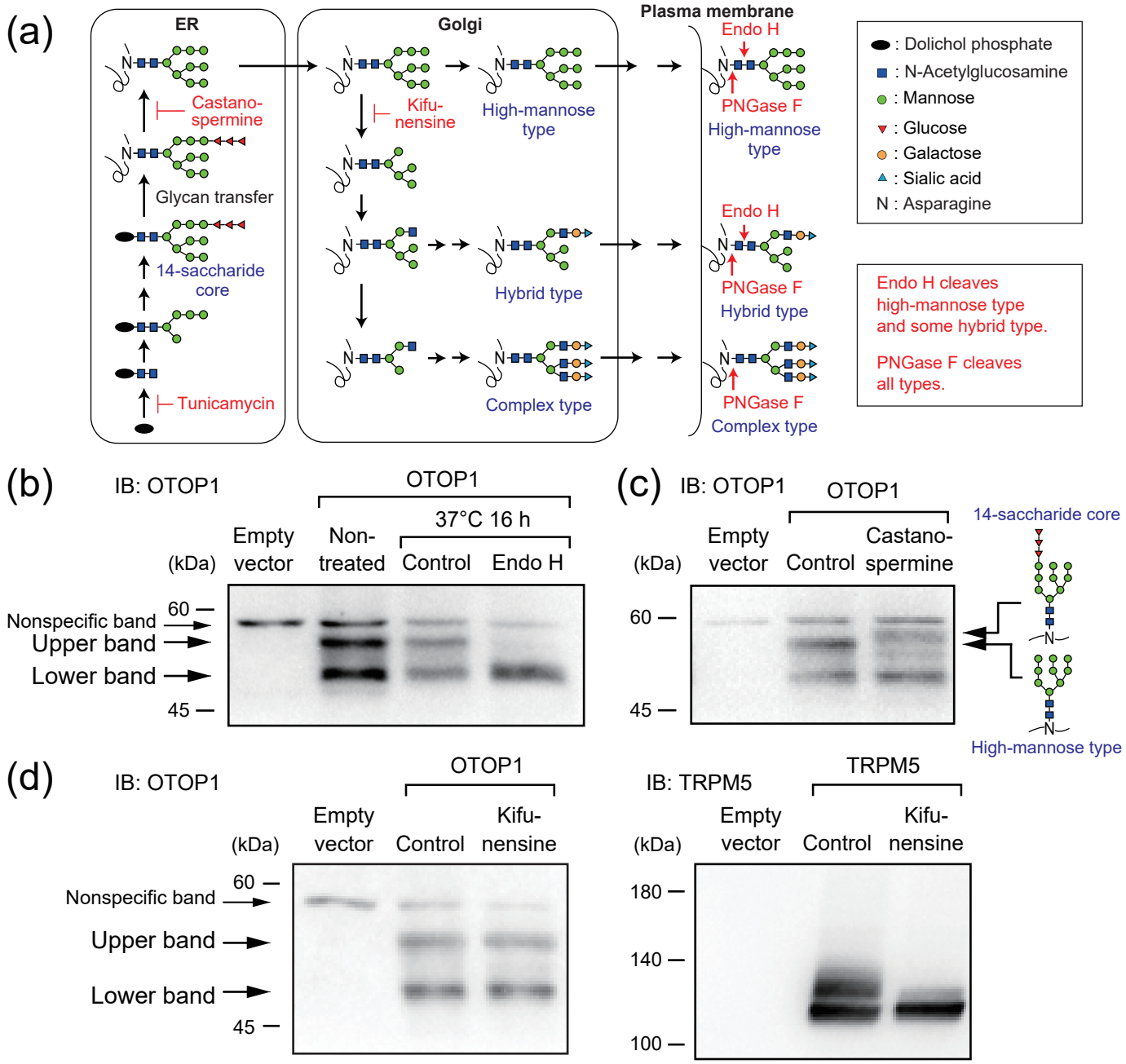

Figure 2

The N-glycans of OTOP1 are most likely high-mannose type. (a) A simplified sequence of N-glycan biosynthesis, and inhibitors and glycosidases of N-glycosylation. Tunicamycin inhibits the formation of N-acetylglucosamine-lipid intermediates. Castanospermine inhibits trimming of initially attached 14-saccharide core, an immature glycan. Kifunensine prevents the formation of hybrid type N-glycan and complex type N-glycan by inhibiting further trimming of mannose from high-mannose type N-glycan. Endo H cleaves high-mannose type N-glycan and some hybrid type N-glycan. PNGase F cleaves all types of N-glycan. (b) A representative result of a treatment with Endo H. After lysis of the OTOP1 expressing cells, the lysates were incubated with 50 U/μl Endo H at 37°C for 16 hours (Endo H) or without it (Control). To confirm the position of the intact OTOP1, which was not exposed by any extra-treatment, the lysate of HEK293T cells expressing OTOP1 (Non-treated) and the lysate of HEK293T cells which were transfected with an empty vector (Empty vector) were loaded. (c) The OTOP1 expressing HEK293T cells were incubated with 100 μg/ml castanospermine, an α/β-glucosidase inhibitor (Castanospermine) or without it (Control) for 30 hours from just before transfection. (d) The OTOP1 expressing HEK293T cells were incubated with 50 μM kifunensine, an inhibitor of class I α-mannosidases (Kifunensine), or without it (Control) for 30 hours from just before transfection, and OTOP1 was detected (left). To confirm that 50 μM kifunensine inhibited class I α-mannosidases of the cells, HA-tagged rat TRPM5 expressing HEK293T cells were incubated with 50 μM kifunensine, and TRPM5 was detected using an anti-HA antibody (right). All experiments were repeated three times.

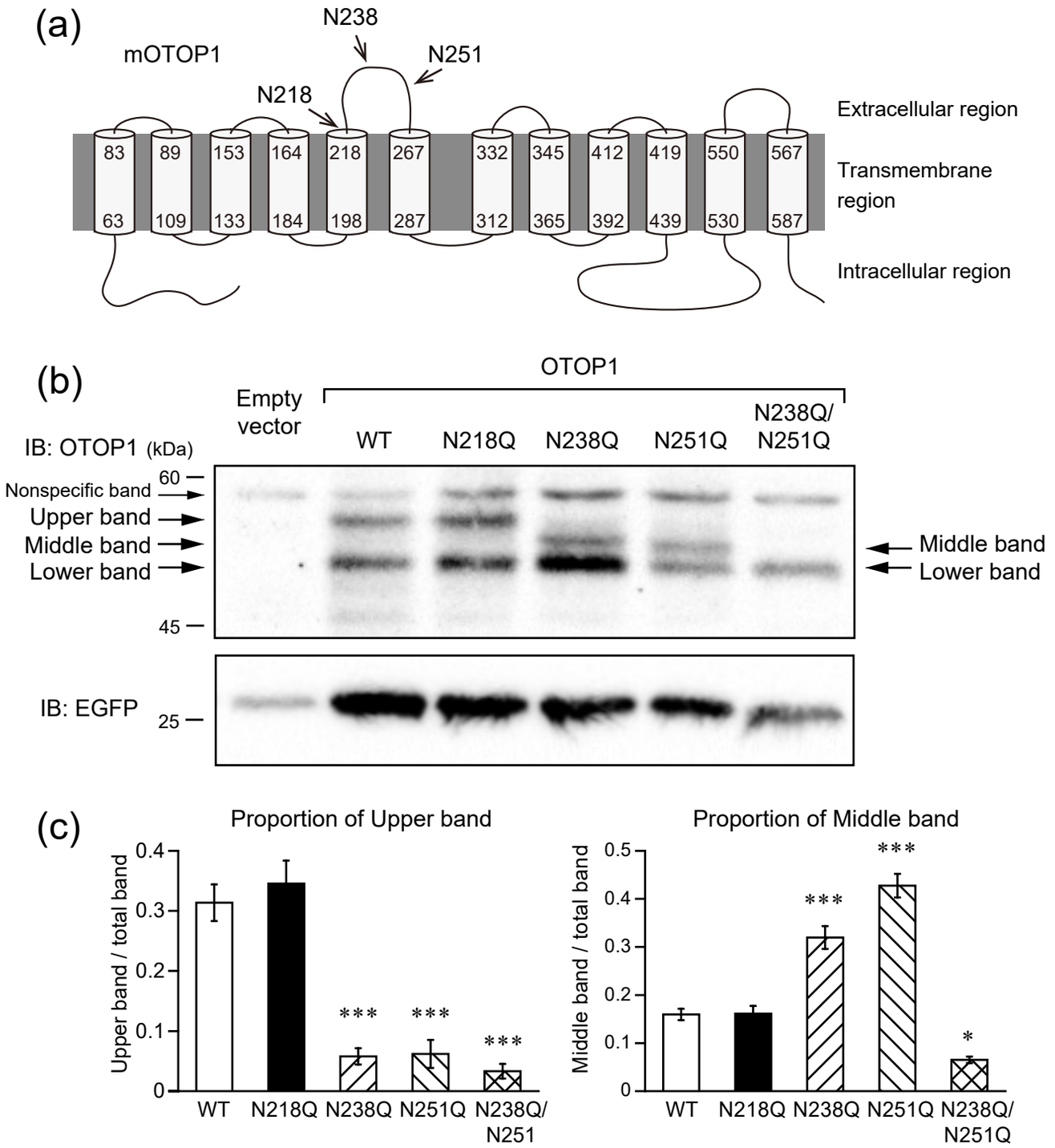

Figure 3

OTOP1 was glycosylated at 238th asparagine residue (N238) and 251st asparagine residue (N251). (a) A membrane topology of OTOP1, which was predicted by TOPCONS (Bernsel et al., 2009). The arrows indicate the positions of three candidate asparagine residues (218th asparagine (N218), N238, and N251) which fulfill the N-glycosylation consensus sequence (Asn-X-Thr/Ser, N-X-T/S, where X is any amino acid residue except proline) in the extracellular region. (b) A representative result (out of three blots) of western blot analysis for OTOP1 (upper) or EGFP (lower). HEK293T cells were transfected with an empty vector (Empty vector) or expressed wild-type OTOP1 (WT), N218Q mutant (N218Q), N238Q mutant (N238Q), N251Q mutant (N251Q), or N238Q and N251Q double mutant (N238Q/N251Q). In addition to Upper band and Lower band, N238Q and N251Q showed Middle band between Upper band and Lower band. (c) The band intensities of Upper band, Middle band, and Lower band of OTOP1 were measured, and the proportions of Upper band (left) or Middle band (right) in WT, N218Q, N238Q, N251Q, and N238Q/N251Q were calculated and illustrated as a bar graph. Shown are mean ± SEM. *: $p < 0.05$, ***: $p < 0.001$ (Dunnett's test, vs WT, n = 3).

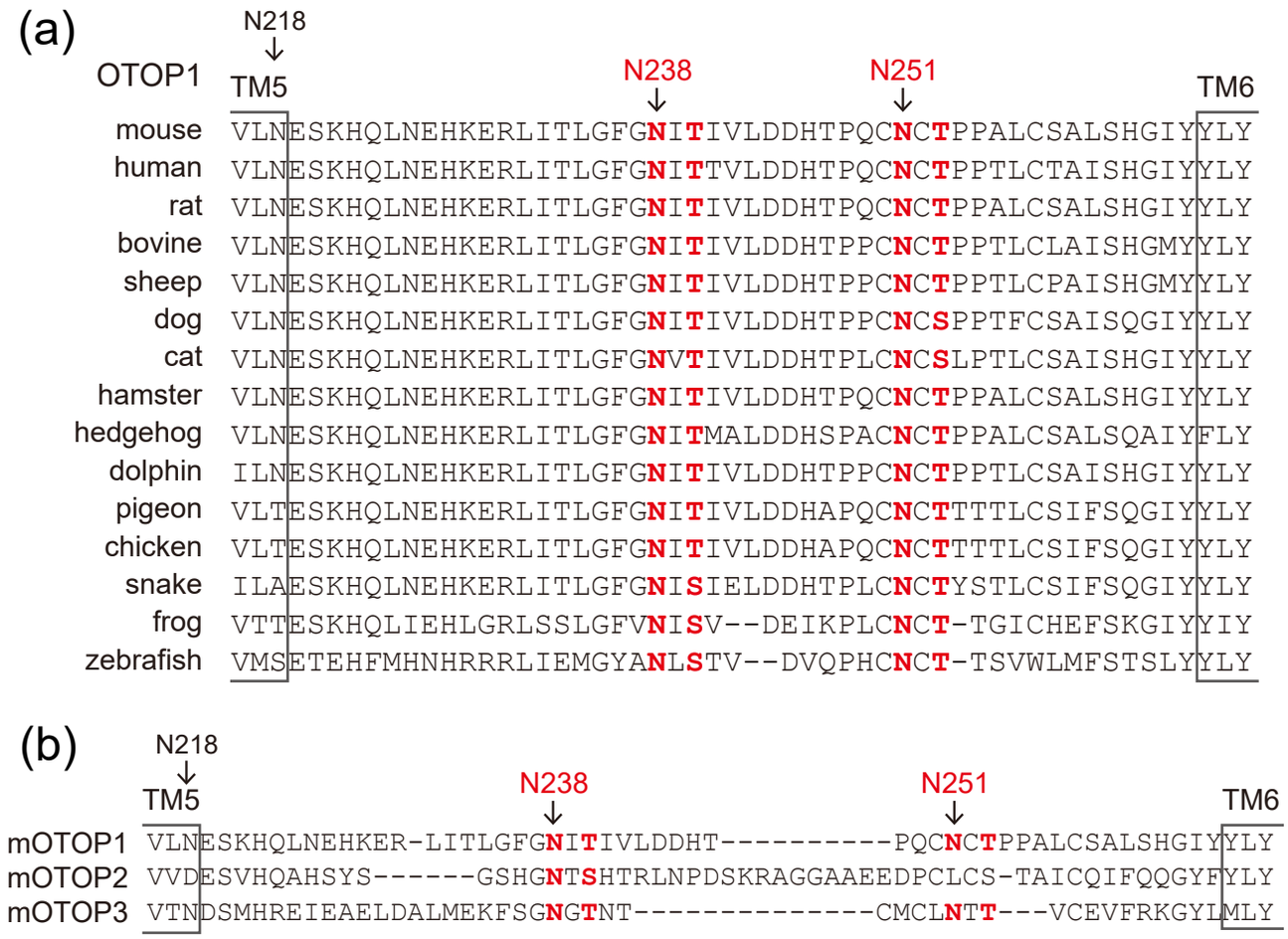

Figure 4

The N-glycosylated asparagine residues (N238 and N251) are conserved in vertebrate OTOP1 and other OTOP family members (OTOP2 and OTOP3). (a) An amino acid sequence alignment of the third extracellular loop between the fifth transmembrane region (TM5) and the sixth transmembrane region (TM6) of several vertebrate OTOP1. Binominal names and Genbank accession numbers of the vertebrate OTOP1 are as follows: mouse: *Mus musculus*; NP_766297.2, human: *Homo sapiens*; NP_819056.1, rat: *Rattus norvegicus*; NP_852098.1, bovine: *Bos taurus*; NP_001193713.1, sheep: *Ovis aries*; XP_014951783.2, dog: *Canis lupus familiaris*; XP_03389628, cat: *Felis catus*; XP_023109080, hamster: *Phodopus roborovskii*; CAH6975926.1, hedgehog: *Erinaceus europaeus*; XP_060044452.1, dolphin: *Lagenorhynchus albirostris*; XP_060003039, pigeon: *Columba livia*; KAK2541027.1, chicken: *Gallus gallus*; XP_040528877.1, snake: *Pantherophis guttatus*; XP_034288795, frog: *Xenopus laevis*; XP_018124006, zebrafish: *Danio rerio*; NP_942098.1. Asparagine (N) and threonine or serine (T/S) which correspond to the consensus sequences of N238 and N251 of mouse OTOP1 are written in red bold letters. (b) An amino acid sequence alignment of the third extracellular loop of mouse OTOP1, mouse OTOP2 (NP_001334576.1), and mouse OTOP3 (NP_001334576.1). N and T/S which correspond to the consensus sequences of N238 and N251 of mouse OTOP1 are written in red bold letters.

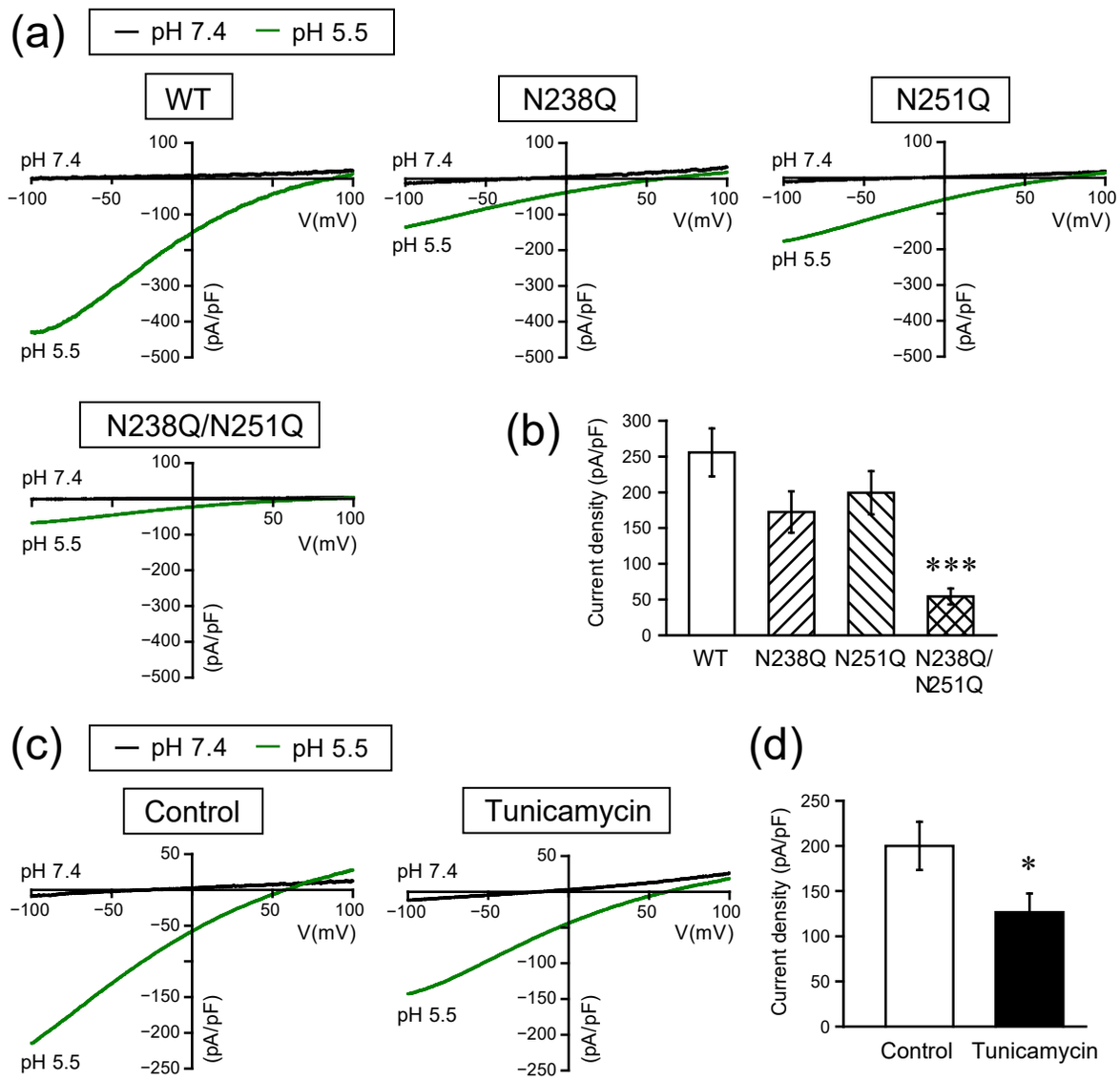

Figure 5

Prevention of glycosylation reduced whole-cell OTOP1 current density. (a) Representative current-voltage (I-V) plots of whole-cell current densities which were measured from HEK293T cells expressing WT OTOP1 or mutant OTOP1 (N238Q, N251Q, and N238Q/N251Q) at pH 7.4 (black line) or pH 5.5 (green line). (b) A summary of current density magnitudes of WT OTOP1 and mutant OTOP1 (N238Q, N251Q, and N238Q/N251Q) at –100 mV, evoked by a pH 5.5 solution [(current density at pH 7.4) – (current density at pH 5.5)]. Shown are mean ± SEM. ***: $p < 0.001$ (Dunnett's test, vs WT, n = 10 to 16). (c) Representative I-V plots of whole-cell OTOP1 current densities which were measured at pH 7.4 (black line) or pH 5.5 (green line) from HEK293T cells treated with 2.0 µg/ml tunicamycin (Tunicamycin) or its solvent, 0.02% DMSO (Control) for 26 hours. (d) A summary of current density magnitudes evoked by a pH 5.5 solution at –100 mV. Cells were treated with tunicamycin (Tunicamycin) or DMSO (Control). Shown are mean ± SEM. *: $p < 0.05$ (unpaired Student's t-test, n = 13 or 14).

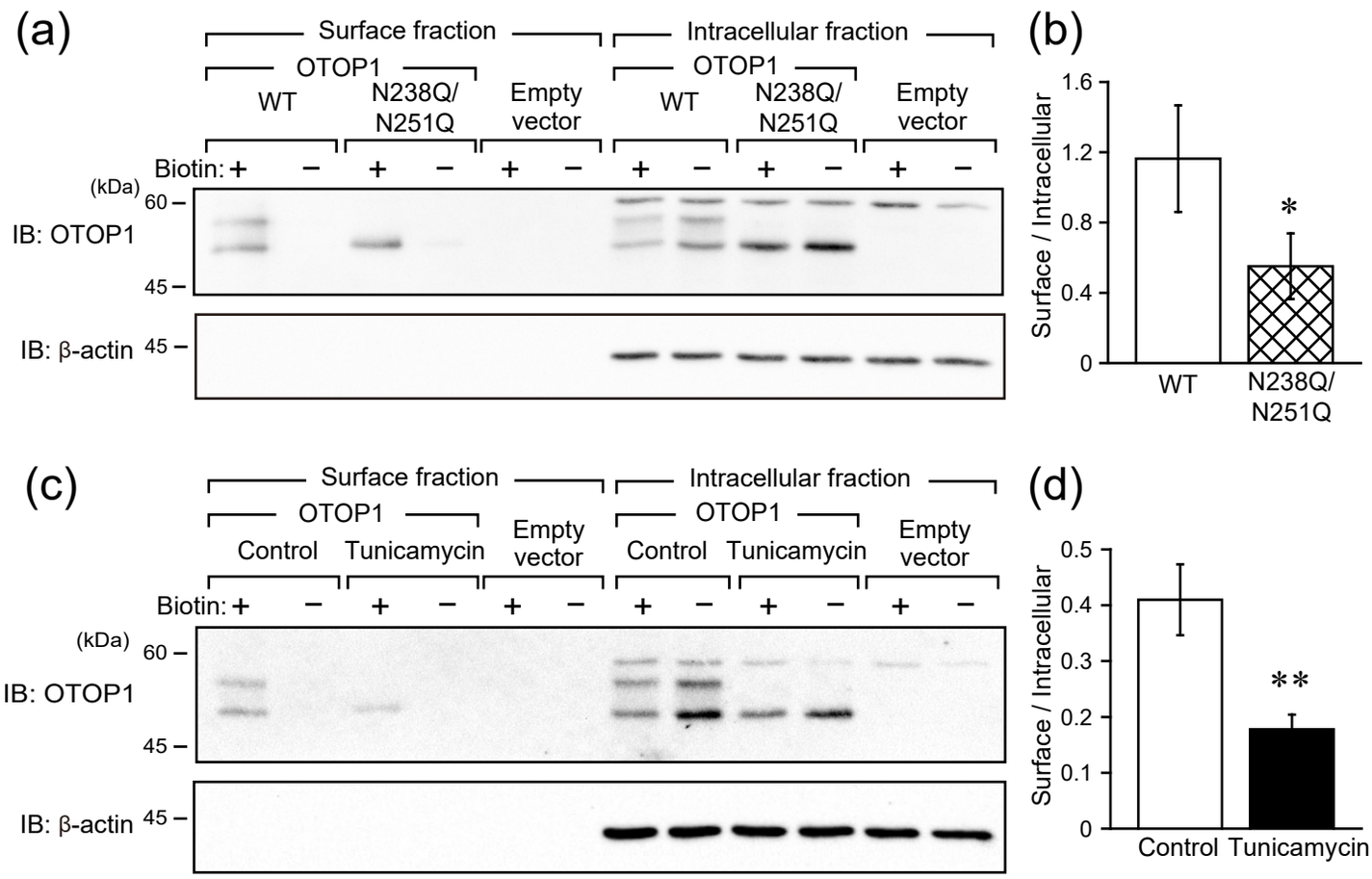

Figure 6

Prevention of glycosylation reduced surface expression of OTOP1. (a) A representative result (out of five blots) of a cell surface biotinylation assay of WT OTOP1 and N238Q/N251Q mutant. The left half of the membrane shows surface fractions, and the right half shows intracellular fractions. HEK293T cells expressed WT OTOP1 or N238Q/N251Q mutant, or were transfected with an empty vector. To monitor nonspecific binding to avidin beads, non-biotinylated cell lysates (Biotin –) were pulled down in addition to biotinylated cell lysates (Biotin +). In the upper membrane, OTOP1 was detected. In the lower membrane, β-actin was detected to confirm negligible leakage of intracellular proteins into the surface fractions. (b) A summary of the ratios of OTOP1 proteins (WT OTOP1 or N238Q/N251Q) in the surface fraction to those in the intracellular fraction. Shown are mean ± SEM. *: $p < 0.05$ (paired t-test, n = 5). (c) A representative result (out of four blots) of a cell surface biotinylation assay of WT OTOP1 in the HEK293T cells which were treated with 2.0 μg/ml tunicamycin (Tunicamycin) or its solvent, 0.02% DMSO (Control), for 26 hours. Others are same in (a). (d) A summary of the signal ratios of OTOP1 proteins in the surface fraction of control cells or tunicamycin-treated cells to OTOP1 proteins in the intracellular fraction. Shown are mean ± SEM. **: $p < 0.01$ (paired t-test, n = 4).

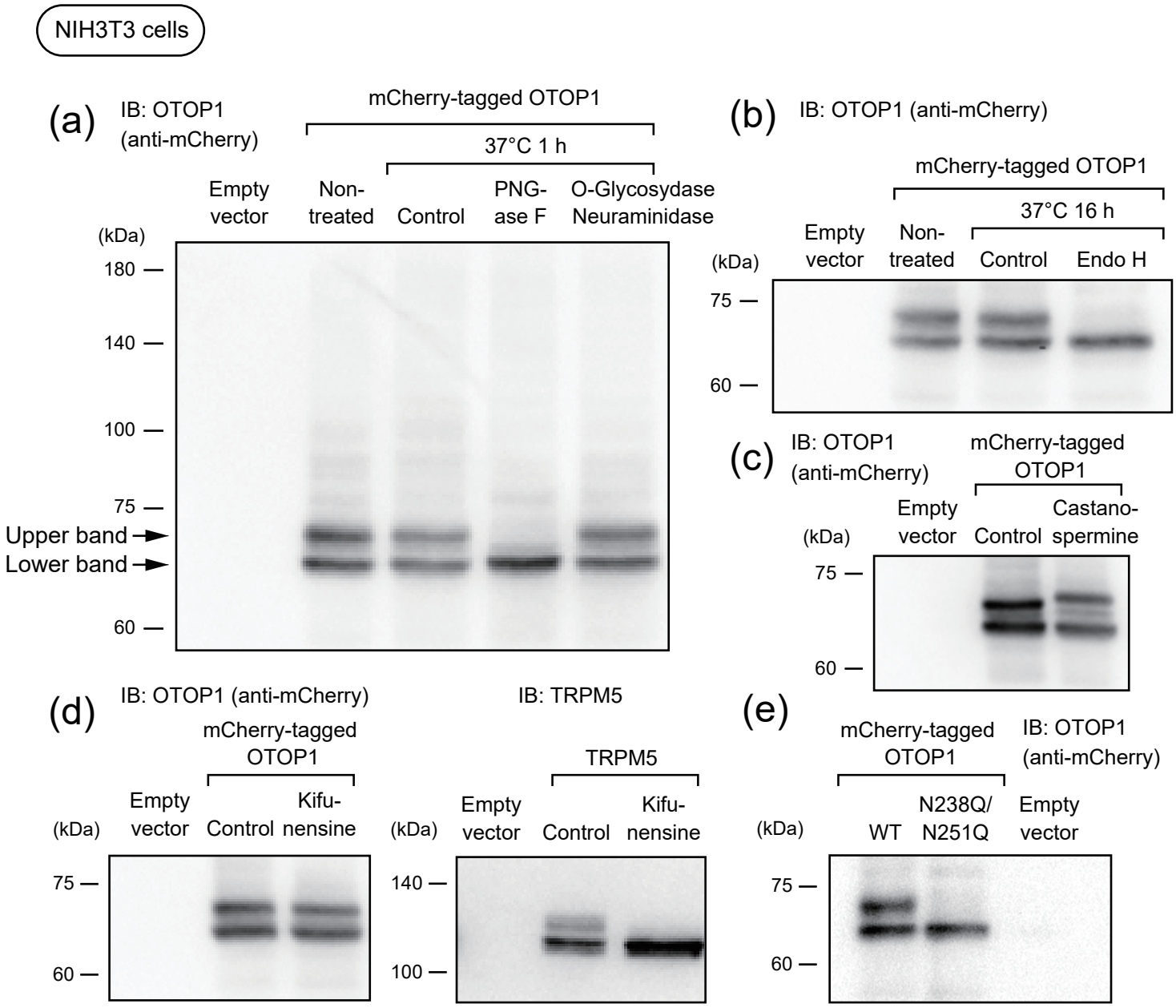

Supporting information S1

OTOP1 was N-glycosylated in NIH3T3 cells, a mouse fibroblast cell line. Each figure is a representative result (out of three blots) of western blot analysis for mCherry-tagged OTOP, which was detected by an anti-mCherry antibody. The lysates of cells which were transfected with an empty vector (pmCherryC1) were loaded as a negative control. The concentrations of drugs and incubation conditions were the same as in the experiments using HEK293T cells. (a) A result of the treatments with enzymes which remove glycans. To confirm the position of the intact mCherry-tagged OTOP1, which was not exposed by any extra-treatment, the lysate of NIH3T3 cells expressing mCherry-tagged OTOP1 (Non-treated) was loaded. The remaining lysates of NIH3T3 expressing mCherry-tagged OTOP1 were treated with distilled water (Control), 25 U/μl peptide:N-glycanase F (PNGase F), or the mixture of 1,000 U/μl O-Glycosidase and 12.5 U/μl Neuraminidase (O-Glycosidase +Neuraminidase) at 37°C for 1 hour. (b) A representative result of treatments with 50 U/μl Endo H, which cleaves the chitobiose core of high mannose-type glycan and a hybrid-type glycan. Others are same in (a). (c) The mCherry-tagged OTOP1 expressing NIH3T3 cells were incubated with 100 μg/ml castanospermine, an α/β-glucosidase inhibitor (Castanospermine) or without it (Control) for 30 hours from just before transfection. (d) The mCherry-tagged OTOP1 expressing NIH3T3 cells were incubated with 50 μM kifunensine, an inhibitor of class I α-mannosidases (Kifunensine), or without it (Control) for 30 hours from just before transfection (left). To confirm that 50 μM kifunensine inhibited class I α-mannosidases of the cells, HA-tagged rat TRPM5 expressing NIH3T3 cells were incubated with 50 μM kifunensine, and rat TRPM5 was detected using an anti-HA antibody (right). (e) The lysates of NIH3T3 cells expressing mCherry-tagged wild-type OTOP1 (WT) or N238Q/N251Q double mutant (N238Q/N251Q) were loaded.

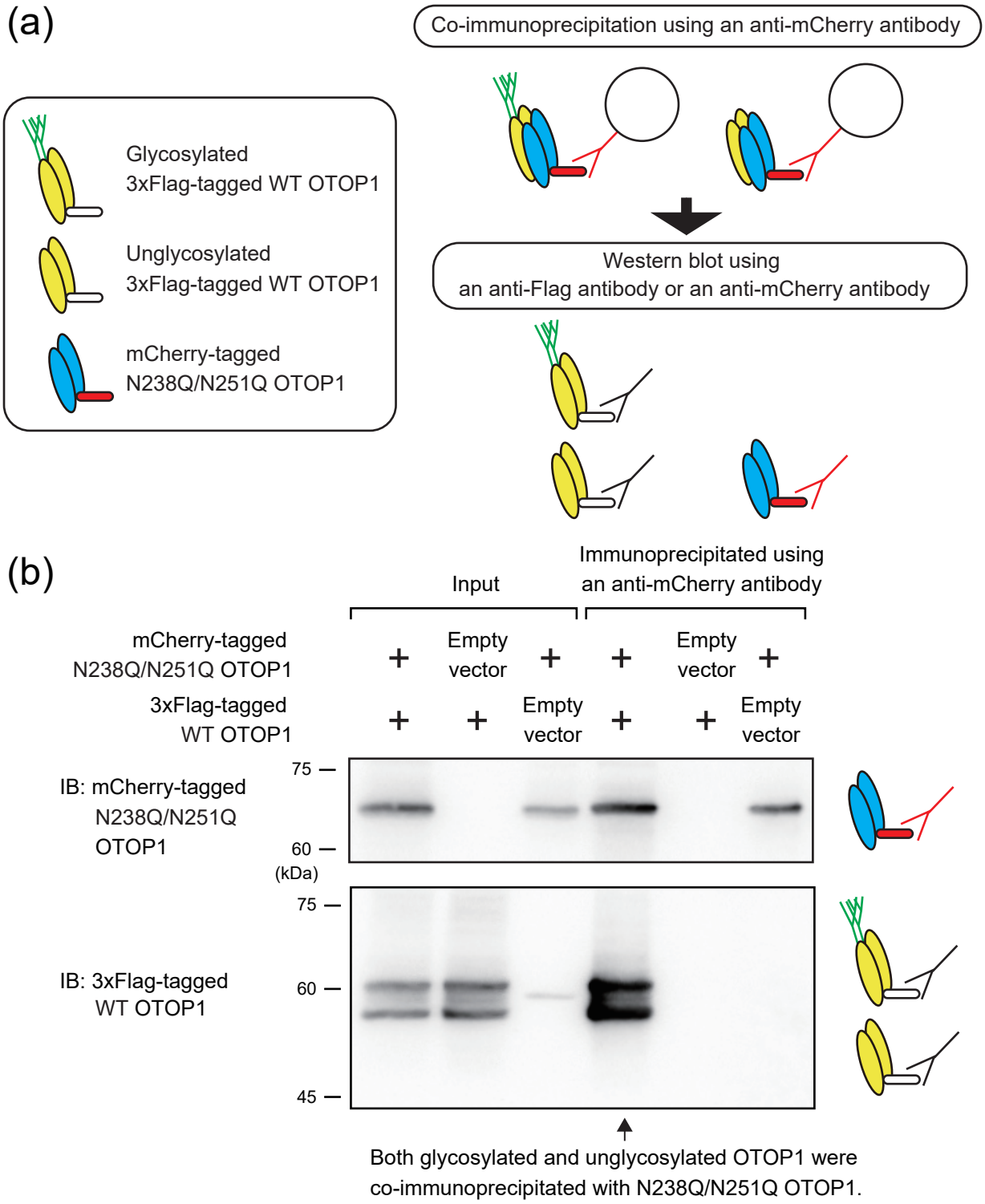

Supporting information S2

Unglycosylated OTOP1 can bind to both glycosylated and unglycosylated OTOP1. (a) Strategy for the detection of the binding between unglycosylated and glycosylated OTOP1. N-terminally mCherry-tagged N238Q/N251Q double mutant OTOP1 and 3×Flag-tagged wild type OTOP1 were coexpressed in HEK293T cells. The mCherry-tagged N238Q/N251Q OTOP1 was immunoprecipitated using an anti-mCherry antibody. If the unglcosylated OTOP1 (N238Q/N251Q OTOP1) can bind with both glycosylated form and unglycosylated form of OTOP1 (3×Flag-tagged OTOP1), both will be detected by western blotting using an anti-Flag antibody. (b) A representative result (out of three blots) of western blot analysis for the co-immunoprecipitation experiment. The pattern of the expressed constructs is indicated above the images of the membranes. The lysates of the cells (input) were loaded on the left half of the membrane, and the precipitates using an anti-mCherry antibody were loaded on the right half of the membrane. On the upper membrane, mCherry-tagged N238Q/N251Q OTOP1 was immunoblotted (IB). On the lower membrane, 3×Flag-tagged wild type OTOP1 was immunoblotted. Both glycosylated and unglycosylated 3×Flag-tagged OTOP1 were co-immunoprecipitated with mCherry-tagged unglycosylated (N238Q/N251Q) OTOP1.

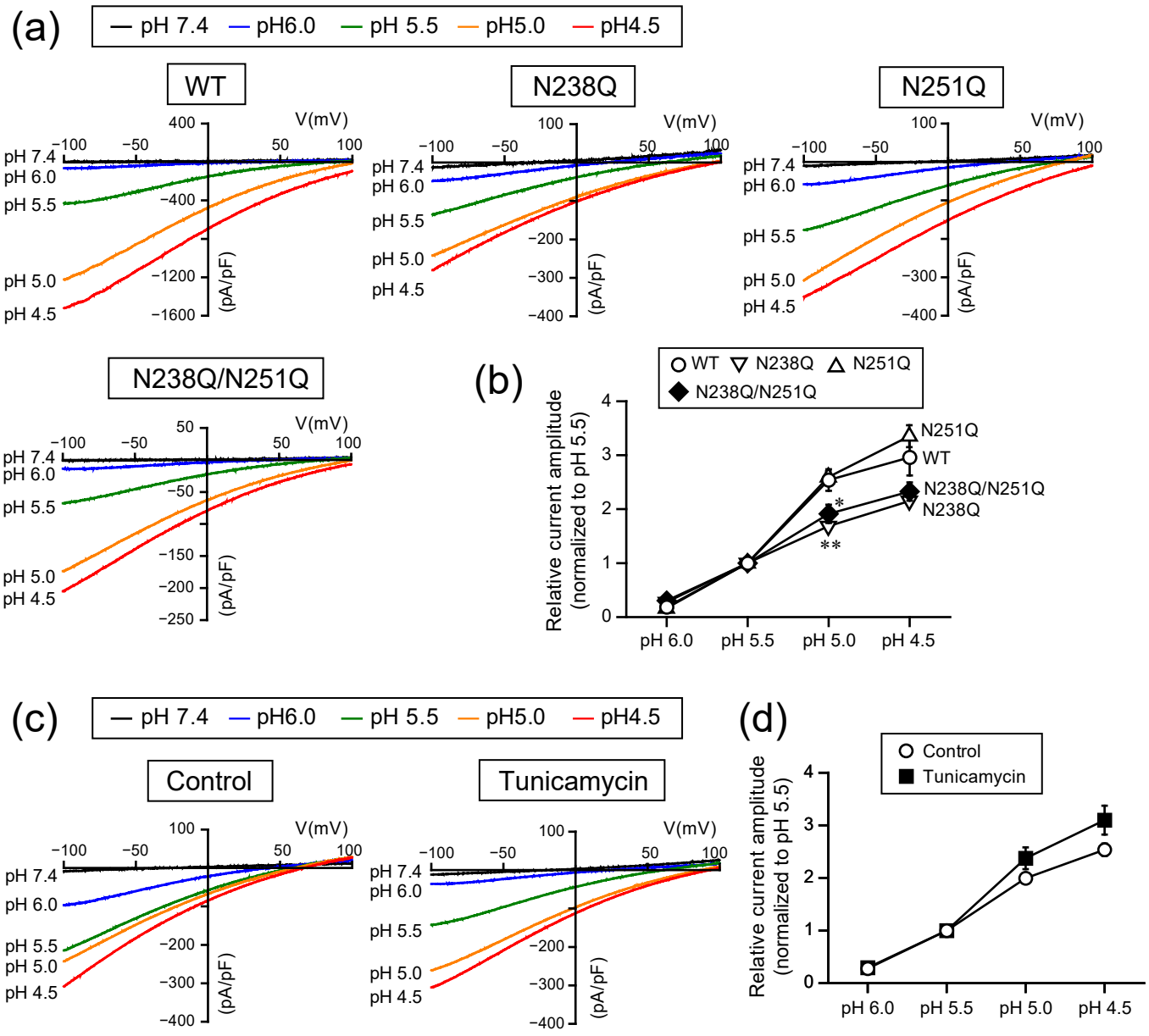

Supporting information S3

The glycosylations did not play a crucial role for the activation of OTOP1 by extracellular acid. (a) Representative current-voltage (I-V) plots of whole-cell current densities which were measured from HEK293T cells expressing WT OTOP1 or mutant OTOP1 (N238Q, N251Q, and N238Q/N251Q) at pH 7.4 (black line), pH 6.0 (blue line), pH 5.5 (green line), pH 5.0 (orange line), or pH 4.5 (red line). The traces at pH 7.4 and pH 5.5 are the same as those in Figure 4(a). (b) A summary of relative current amplitudes at –100 mV at pH 6.0, pH 5.0, and pH 4.5, which were normalized to the current amplitude at pH 5.5. WT OTOP1: circle, N238Q mutant: inverted triangle, N251Q mutant: triangle, N238Q/N251Q mutant: diamond. Shown are mean ± SEM *: $p < 0.05$, **: $p < 0.01$ (Dunnett's test, vs WT, n = 4 to 9). (c) Representative I-V plots of whole-cell OTOP1 current densities which were measured at pH 7.4 (black line), pH 6.0 (blue line), pH 5.5 (green line), pH 5.0 (orange line), or pH 4.5 (red line) from HEK293T cells treated with 2.0 µg/ml tunicamycin (Tunicamycin) or its solvent, 0.02% DMSO (Control). The traces at pH 7.4 and pH 5.5 are the same as those in Figure 4c. (d) A summary of relative current amplitudes at –100 mV at pH 6.0, pH 5.0, and pH 4.5, which were normalized to the current amplitude at pH 5.5. DMSO-treated cells (Control): circle, tunicamycin-treated cells (Tunicamycin): square. Shown are mean ± SEM. There was no significant difference between Control and Tunicamycin at any pH (unpaired Student's t-test, n = 3 to 5).